

DFTT 48/95
hep-ph/9508277

ELASTIC νN AND $\bar{\nu} N$ SCATTERING AND STRANGE FORM FACTORS OF THE NUCLEONS

W.M. Alberico^a, S.M. Bilenky^{a,b}, C. Giunti^a and C. Maieron^a

^a*INFN, Sezione di Torino and Dipartimento di Fisica Teorica, Università di Torino,
Via P. Giuria 1, 10125 Torino, Italy*

^b*Joint Institute for Nuclear Research, Dubna, Russia*
(April 26, 2018)

Abstract

Elastic scattering of neutrinos and antineutrinos on nucleons is considered. It is shown that the measurement of the neutrino-antineutrino asymmetry would allow to obtain model independent informations on the strange axial and vector form factors. The ratio of the magnetic form factors of the proton and neutron, on which the asymmetry depends, is investigated in detail. The asymmetry is calculated under different assumptions on the behavior of the strange vector and axial form factors.

I. INTRODUCTION

The measurement performed by the EMC collaboration [1] of the polarized structure function of the proton g_1^p led to a big progress in the investigation of the structure of the nucleon (see Ref. [2]). One of the conclusions based on the EMC data was that the value of the one-nucleon matrix element of the strange axial current is comparable with those of the u and d axial currents. The latest experiments done at CERN [3] and SLAC [4] confirm this conclusion.

The one-nucleon matrix element of the axial quark current has the following form:

$$\langle p, s | \bar{q} \gamma^\alpha \gamma_5 q | p, s \rangle = 2Ms^\alpha g_A^q. \quad (1.1)$$

Here p is the nucleon momentum, M is the nucleon mass, s^α is the spin vector and g_A^q is a constant.

The constants g_A^u , g_A^d and g_A^s can be determined from the following three constraints:

1. The QCD sum rule [5,2]

$$\Gamma_1^p = \int_0^1 g_1^p dx = \frac{1}{2} \left(\frac{4}{9} g_A^u + \frac{1}{9} g_A^d + \frac{1}{9} g_A^s \right) \left(1 - \frac{\alpha_s}{\pi} + \dots \right), \quad (1.2)$$

Here α_s is the QCD coupling constant.

2. The relation

$$g_A = g_A^u - g_A^d, \quad (1.3)$$

where the constant $g_A = 1.2573 \pm 0.0028$ is the axial constant, which is determined from neutron decay.

3. The relation

$$3F - D = g_A^u + g_A^d - 2g_A^s. \quad (1.4)$$

The values of the constants F and D can be determined from semileptonic decays of hyperons. From the latest data it follows [6]: $F = 0.459 \pm 0.008$ and $D = 0.798 \pm 0.008$.

The relation (1.3) is based on isotopic SU(2) invariance. The relation (1.4) is derived from exact SU(3) invariance.

From the data of the latest experiments [3,4] on the measurement of g_1^p it has been found that

$$\begin{aligned} \Gamma_1^p &= 0.133 \pm 0.04 \pm 0.012 & (\text{E143}), \\ \Gamma_1^p &= 0.136 \pm 0.011 \pm 0.011 & (\text{SMC}). \end{aligned} \quad (1.5)$$

The global fit of all data gives [7]

$$\begin{aligned} g_A^u &= 0.83 \pm 0.03 \\ g_A^d &= -0.43 \pm 0.03 \\ g_A^s &= -0.10 \pm 0.03 \end{aligned} \quad (1.6)$$

Thus, the value of the constant g_A^s , that characterizes the matrix element of the strange axial current, is comparable with those of the constants g_A^u and g_A^d . This fact has brought a lot of discussions in the literature (see Ref. [2]).

In the parton model the constants g_A^q are easily calculated. The result is well known:

$$g_A^q = \Delta q \equiv \int_0^1 \left(\sum_r r q^r(x) + \sum_r r \bar{q}^r(x) \right) dx , \quad (1.7)$$

where $q^r(x)$ ($\bar{q}^r(x)$) is the density of quarks q (antiquarks \bar{q}) with momentum fraction x and helicity r .

Thus, in the parton model, the constant g_A^q is the contribution of q (and \bar{q}) to the helicity of proton. In the parton model the total contribution of the u , d and s quarks (and antiquarks) to the helicity of the proton is given by

$$\sum_{q=u,d,s} \Delta q = \sum_{q=u,d,s} g_A^q . \quad (1.8)$$

From the analysis of the EMC data it was obtained that the averaged value of the constant $\sum_{q=u,d,s} g_A^q$ is close to zero. That was the origin of the “problem of the spin of the proton”.

One way of solving this problem was the calculation of the contribution of gluons to the helicity of the proton. It was shown [8] that, due to the triangle anomaly, this contribution can be large. According to the latest data $\sum_{q=u,d,s} g_A^q = 0.31 \pm 0.07$.

The values of the constants g_A^q given in Eq.(1.6) were obtained under several assumptions. The calculation of the quantity Γ_1^p that enter in the QCD sum rule (1.2) requires the extrapolation of the experimental data in the region of small x . The value of the integral Γ_1^p depends significantly on the assumptions on the behaviour of the function $g_1^p(x)$ at small x . In some models (see, for example, Refs. [7,9]) this function can have a singularity at $x = 0$. Another important assumption is the exact SU(3) symmetry. It was shown in Ref. [10] that a violation of the SU(3) symmetry can change strongly the numerical value of the constant g_A^s .

It is then clear that it is very important to use other methods for the determination of the matrix elements of the strange current. The investigation of neutral-current (NC) neutrino reactions is one of these ways [11]. We will consider here the elastic scattering of muon neutrinos and antineutrinos on nucleons:

$$\nu_\mu + N \rightarrow \nu_\mu + N , \quad (1.9)$$

$$\bar{\nu}_\mu + N \rightarrow \bar{\nu}_\mu + N . \quad (1.10)$$

The cross sections of these processes depend on the electromagnetic form factors, on the axial form factor and on the strange axial and vector form factors of the nucleon. As it was shown in Ref. [12], the value of the constant g_A^s that can be extracted from the cross sections of the processes (1.9) and (1.10) strongly depends on the behaviour of the axial form factor, which is rather poorly known. In order to minimize this dependence we will consider here

the asymmetry

$$\mathcal{A}_N(Q^\epsilon) = \frac{\left(\frac{d\sigma}{dQ^2}\right)_{\nu N}^{\text{NC}} - \left(\frac{d\sigma}{dQ^2}\right)_{\bar{\nu} N}^{\text{NC}}}{\left(\frac{d\sigma}{dQ^2}\right)_{\nu \setminus}^{\text{CC}} - \left(\frac{d\sigma}{dQ^2}\right)_{\bar{\nu} \setminus}^{\text{CC}}}, \quad (1.11)$$

where $\left(\frac{d\sigma}{dQ^2}\right)_{\nu N}^{\text{NC}}$ and $\left(\frac{d\sigma}{dQ^2}\right)_{\bar{\nu} N}^{\text{NC}}$ are the cross sections of the processes (1.9) and (1.10), respectively, while $\left(\frac{d\sigma}{dQ^2}\right)_{\nu n}^{\text{CC}}$ and $\left(\frac{d\sigma}{dQ^2}\right)_{\bar{\nu} p}^{\text{CC}}$ are, respectively, the cross sections of the quasi-elastic charged-current (CC) processes

$$\nu_\mu + n \rightarrow \mu^- + p, \quad (1.12)$$

$$\bar{\nu}_\mu + p \rightarrow \mu^+ + n. \quad (1.13)$$

Here $Q^2 \equiv -q^2$, where $q = p' - p$, p and p' are the momenta of the initial and final nucleons, respectively.

We will show that measurements of the asymmetry $\mathcal{A}_N(Q^\epsilon)$ will allow to obtain model independent informations on the strange axial and vector form factors of the nucleon.

Let us conclude this introduction with the following remark. The last experiment on the measurement of the cross sections of elastic NC scattering of neutrinos and antineutrinos on protons was done about 10 years ago in BNL [13]. We think that now it is a proper time to continue these investigations. A wide program of long-baseline neutrino experiments are under preparation and under discussion at the moment [14]. The main aim of these experiments is to search for neutrino oscillations in a distant detector. A detector will be placed near the neutrino source for the calibration of the beam. This detector will register a large number of neutrino events. Taking into account the importance of the knowledge of the strange form factors of the nucleon, we think that the possibility to perform a measurement of the cross section of elastic scattering of neutrinos and antineutrinos on nucleons in the “near” detector should be considered seriously.

II. THE ASYMMETRY

Let us consider the elastic scattering of ν_μ and $\bar{\nu}_\mu$ on nucleons. The standard effective Hamiltonian for these processes is given by

$$\mathcal{H}_I^{\text{NC}} = \frac{\mathcal{G}}{\sqrt{\epsilon}} \bar{\nu}_\mu \gamma^\alpha (\infty + \gamma_\nabla) \nu_\mu |_\alpha^Z, \quad (2.1)$$

where the neutral current j_α^Z can be written in the form

$$j_\alpha^Z = v_\alpha^3 + a_\alpha^3 - 2 \sin^2 \theta_W j_\alpha^{\text{em}} - \frac{1}{2} v_\alpha^s - \frac{1}{2} a_\alpha^s \quad (2.2)$$

Here j_α^{em} is the electromagnetic current, v_α^3 and a_α^3 are the third components of the isovector vector and axial currents

$$v_\alpha^i = \bar{N} \gamma_\alpha \frac{\tau^i}{2} N, \quad (2.3)$$

$$a_\alpha^i = \bar{N} \gamma_\alpha \gamma_5 \frac{\tau^i}{2} N, \quad (2.4)$$

$(N = \begin{pmatrix} u \\ d \end{pmatrix})$ is the SU(2) doublet) and

$$v_\alpha^s = \bar{s} \gamma_\alpha s, \quad (2.5)$$

$$a_\alpha^s = \bar{s} \gamma_\alpha \gamma_5 s \quad (2.6)$$

are the strange vector and axial currents. In Eq.(2.2) we kept only the contribution to the neutral current of the light u , d and s quarks.

The one-nucleon matrix element of the neutral current has the following general form

$$\langle p' | J_\alpha^Z | p \rangle = \bar{u}(p') \left[\gamma_\alpha F_V^Z(Q^2) + \frac{i}{2M} \sigma_{\alpha\beta} q^\beta F_M^Z(Q^2) + \gamma_\alpha \gamma_5 F_A^Z(Q^2) \right] u(p). \quad (2.7)$$

From Eq.(2.2), for the vector NC form factors we have

$$(F_V^Z)_{p(n)} = \pm F_1^3 - 2 \sin^2 \theta_W F_1^{p(n)} - \frac{1}{2} F_V^s, \quad (2.8)$$

$$(F_M^Z)_{p(n)} = \pm F_2^3 - 2 \sin^2 \theta_W F_2^{p(n)} - \frac{1}{2} F_M^s. \quad (2.9)$$

Here $F_1^{p(n)}$ and $F_2^{p(n)}$ are the Dirac and Pauli electromagnetic form factors of the proton (neutron), F_V^s and F_M^s are the strange vector form factors and $F_{1,2}^3$ are the isovector form factors of the nucleon. From isotopic invariance it follows that

$$F_{1,2}^3 = \frac{1}{2} (F_{1,2}^p - F_{1,2}^n) \quad (2.10)$$

Furthermore, using the isotopic SU(2) invariance of strong interactions we have

$${}_p \langle p' | A_\alpha^3 | p \rangle_p = - {}_n \langle p' | A_\alpha^3 | p \rangle_n = \frac{1}{2} {}_p \langle p' | A_\alpha^{1+i2} | p \rangle_n, \quad (2.11)$$

$A_\alpha^{1+i2} = A_\alpha^1 + i A_\alpha^2$ being the charged axial current. From Eq.(2.2) we obtain

$$(F_A^Z)_{p(n)} = \pm \frac{1}{2} F_A - \frac{1}{2} F_A^s. \quad (2.12)$$

where F_A is the CC axial form factor and F_A^s is the axial strange form factor.

Using Eqs.(2.8), (2.9) and (2.12), for the difference of cross sections of the NC processes (1.9) and (1.10) we obtain the following expression:

$$\begin{aligned} \left(\frac{d\sigma}{dQ^2} \right)_{\nu p(n)}^{\text{NC}} - \left(\frac{d\sigma}{dQ^2} \right)_{\bar{\nu} p(n)}^{\text{NC}} &= \frac{G^2}{\pi} \frac{Q^2}{p \cdot k} \left(1 - \frac{Q^2}{4p \cdot k} \right) \\ &\times \left(\pm G_M^3 - 2 \sin^2 \theta_W G_M^{p(n)} - \frac{1}{2} G_M^s \right) \left(\pm \frac{1}{2} F_A - \frac{1}{2} F_A^s \right) \end{aligned} \quad (2.13)$$

where k is the momentum of the initial neutrino, $G_M^{p(n)} = F_1^{p(n)} + F_2^{p(n)}$ is magnetic form factor of the proton (neutron), $G_M^3 = \frac{1}{2}(G_M^p - G_M^n)$ is the isovector magnetic form factor and $G_M^s = F_V^s + F_M^s$ is the strange magnetic form factor.

Let us consider now the quasi-elastic CC processes (1.12) and (1.13). The standard effective Hamiltonian for these processes is given by

$$\mathcal{H}_{\mathcal{I}}^{\text{CC}} = \frac{\mathcal{G}}{\sqrt{\epsilon}} \bar{\mu} \gamma^\alpha (\infty + \gamma_\nabla) \nu_\mu |_\alpha + \text{h.c.} \quad (2.14)$$

Here

$$j_\alpha = [\bar{u} \gamma^\alpha (1 + \gamma_5) d] V_{ud} = [v_\alpha^{1+i2} + a_\alpha^{1+i2}] V_{ud} \quad (2.15)$$

is the hadronic charged current and V_{ud} is the element of C-K-M mixing matrix. The one-nucleon matrix element of the CC has the form

$$\begin{aligned} {}_p \langle p' | J_\alpha^{1+i2} | p \rangle_n &= {}_n \langle p' | J_\alpha^{1-i2} | p \rangle_p \\ &= \bar{u}(p') \left[\gamma_\alpha F_V(Q^2) + \frac{i}{2M} \sigma_{\alpha\beta} q^\beta F_M(Q^2) + \gamma_\alpha \gamma_5 F_A(Q^2) \right] u(p) . \end{aligned} \quad (2.16)$$

From isotopic SU(2) invariance it follows that

$$\begin{aligned} F_V &= F_1^p - F_1^n = 2 F_1^3 \\ F_M &= F_2^p - F_2^n = 2 F_2^3 \end{aligned} \quad (2.17)$$

Using Eq.(2.17), for the difference of cross sections of the CC processes (1.12) and (1.13) we obtain

$$\left(\frac{d\sigma}{dQ^2} \right)_{\nu n}^{\text{CC}} - \left(\frac{d\sigma}{dQ^2} \right)_{\bar{\nu} p}^{\text{CC}} = \frac{G^2}{\pi} \frac{Q^2}{p \cdot k} \left(1 - \frac{Q^2}{4p \cdot k} \right) 2 G_M^3 F_A |V_{ud}|^2 \quad (2.18)$$

Finally, from Eqs.(2.13) and (2.18), for the asymmetries $\mathcal{A}_{\sqrt{\epsilon}}$ determined by the expression (1.11) we find the following expression:

$$\mathcal{A}_{\sqrt{\epsilon}} = \frac{\infty}{\Delta |\mathcal{V}_{\nabla}|^\epsilon} \left(\pm \infty - \frac{\mathcal{F}_{\mathcal{A}}^f}{\mathcal{F}_{\mathcal{A}}} \right) \left(\pm \infty - \in \sin^\epsilon \theta_W \frac{\mathcal{G}_{\mathcal{M}}^{\sqrt{\epsilon}}}{\mathcal{G}_{\mathcal{M}}^\epsilon} - \frac{\mathcal{G}_{\mathcal{M}}^f}{\epsilon \mathcal{G}_{\mathcal{M}}^\epsilon} \right) . \quad (2.19)$$

Taking into account only the terms which depend linearly on the strange form factors, we can rewrite Eq.(2.19) in the form

$$R_{p(n)}(Q^2) \mathcal{A}_{\sqrt{\epsilon}}(\mathcal{Q}^\epsilon) = \infty \mp \frac{\mathcal{F}_{\mathcal{A}}^f(\mathcal{Q}^\epsilon)}{\mathcal{F}_{\mathcal{A}}(\mathcal{Q}^\epsilon)} \mp \frac{\infty}{\forall |\mathcal{V}_{\nabla}|^\epsilon} \mathcal{R}_{\sqrt{\epsilon}}(\mathcal{Q}^\epsilon) \frac{\mathcal{G}_{\mathcal{M}}^f(\mathcal{Q}^\epsilon)}{\mathcal{G}_{\mathcal{M}}^\epsilon(\mathcal{Q}^\epsilon)} , \quad (2.20)$$

where the quantity

$$R_{p(n)}(Q^2) = \frac{4 |V_{ud}|^2}{1 \mp 2 \sin^2 \theta_W \frac{G_M^{p(n)}(Q^2)}{G_M^3(Q^2)}} \quad (2.21)$$

is determined by the electromagnetic form factors of the nucleon. Thus, the measurement of the asymmetry $\mathcal{A}_{\sqrt{\lambda}}(\mathcal{Q}^\epsilon)$ would allow to obtain informations about the strange axial and vector form factors directly from the experimental data. If it will turn out that the left-hand side of Eq.(2.20), in which only measurable quantities enter, is different from 1, it will be a model independent proof that the strange nucleon form factors are different from zero.

In neutrino experiments usually the interactions of neutrinos with nuclei are detected. From Eq.(2.13), for the asymmetry averaged over the proton and neutron we obtain the following relation:

$$r \mathcal{A}(\mathcal{Q}^\epsilon) = \infty + \frac{\nabla \sin^\epsilon \theta_W}{\in \left| \mathcal{V}_{\text{p}f} \right|^\epsilon} \frac{\mathcal{G}'_M(\mathcal{Q}^\epsilon)}{\mathcal{G}^3_M(\mathcal{Q}^\epsilon)} \frac{\mathcal{F}_A^f(\mathcal{Q}^\epsilon)}{\mathcal{F}_A(\mathcal{Q}^\epsilon)}, \quad (2.22)$$

where

$$r = \frac{4 |V_{ud}|^2}{1 - 2 \sin^2 \theta_W} \quad (2.23)$$

and $G_M^0 = \frac{1}{2} (G_M^p + G_M^n)$ is the isoscalar magnetic form factor of the nucleon. It is obvious that the interference of the isoscalar strange vector form factor G_M^s and the isovector axial form factor F_A vanishes after averaging over p and n . Thus, the averaged asymmetry $\mathcal{A}(\mathcal{Q}^\epsilon)$ is determined only by the axial strange form factor F_A^s .

The electromagnetic form factors of the nucleon enter into the expression for the asymmetry $\mathcal{A}_{\sqrt{\lambda}}(\mathcal{Q}^\epsilon)$ in the form of the ratio $G_M^{p(n)}/G_M^3$. As it is well known, the electromagnetic form factors satisfy the approximate scaling relations

$$\begin{aligned} G_M^p(Q^2) &= \mu_p G_E^p(Q^2), \\ G_M^n(Q^2) &= \mu_n G_E^p(Q^2), \end{aligned} \quad (2.24)$$

where $\mu_{p(n)}$ is the total magnetic moment of the proton (neutron) in nuclear Bohr magnetons.

Using the values [15]

$$\begin{aligned} \mu_p &= 2.793, & \mu_n &= -1.913, \\ \sin^2 \theta_W &= 0.232, & |V_{ud}| &= 0.975, \end{aligned} \quad (2.25)$$

for the asymmetries $\mathcal{A}_{\sqrt{\lambda}}$, \mathcal{A}_{λ} and the averaged asymmetry \mathcal{A} we obtain the following expressions in the scaling approximation:

$$R_p \mathcal{A}_{\sqrt{\lambda}}(\mathcal{Q}^\epsilon) = \infty - \frac{\mathcal{F}_A^f(\mathcal{Q}^\epsilon)}{\mathcal{F}_A(\mathcal{Q}^\epsilon)} - \infty \infty \infty \frac{\mathcal{G}_M^f(\mathcal{Q}^\epsilon)}{\mathcal{G}_M^3(\mathcal{Q}^\epsilon)}, \quad (2.26)$$

$$R_n \mathcal{A}_{\lambda}(\mathcal{Q}^\epsilon) = \infty + \frac{\mathcal{F}_A^f(\mathcal{Q}^\epsilon)}{\mathcal{F}_A(\mathcal{Q}^\epsilon)} + \infty \infty \infty \frac{\mathcal{G}_M^f(\mathcal{Q}^\epsilon)}{\mathcal{G}_M^3(\mathcal{Q}^\epsilon)}, \quad (2.27)$$

$$r \mathcal{A}(\mathcal{Q}^\epsilon) = \infty + \infty \infty \infty \frac{\mathcal{F}_A^f(\mathcal{Q}^\epsilon)}{\mathcal{F}_A(\mathcal{Q}^\epsilon)}, \quad (2.28)$$

where $R_p = 8.46$, $R_n = 6.11$ and $r = 7.09$. Thus, the asymmetries $\mathcal{A}_{\sqrt{\langle \rangle}}$ are rather sensitive to the axial and vector strange form factors. It is seen from Eqs.(2.26) and (2.27) that the asymmetries $\mathcal{A}_{\sqrt{\langle \rangle}}(\mathcal{Q}^\epsilon)$ have approximately the same sensitivity to the axial and vector strange form factors. The contribution of the axial strange form factor to the averaged asymmetry $\mathcal{A}(\mathcal{Q}^\epsilon)$ is suppressed due to the smallness of the isoscalar part of the magnetic moment of the nucleon with respect to its isovector part.

We calculated also the integral asymmetry

$$\mathbb{A}_N = \frac{\sigma_{\nu N}^{NC} - \sigma_{\bar{\nu} N}^{NC}}{\sigma_{\nu \times}^{CC} - \sigma_{\bar{\nu} \times}^{CC}}, \quad (2.29)$$

where $\sigma_{\nu N}^{NC}$, $\sigma_{\bar{\nu} N}^{NC}$, $\sigma_{\nu \times}^{CC}$ and $\sigma_{\bar{\nu} \times}^{CC}$ are the total cross sections of the processes (1.9), (1.10), (1.12) and (1.13), respectively. From Eqs.(2.13) and (2.18) we have

$$\begin{aligned} \mathbb{A}_{\langle \times \rangle} = & \frac{1}{4|V_{ud}|^2} \left[1 \mp 2 \sin^2 \theta_W \frac{\int dQ^2 X(Q^2) F_A(Q^2) G_M^{p(n)}(Q^2)}{\int dQ^2 X(Q^2) F_A(Q^2) G_M^3(Q^2)} \right. \\ & \mp \frac{\int dQ^2 X(Q^2) F_A^s(Q^2) G_M^3(Q^2) \left(1 \mp 2 \sin^2 \theta_W \frac{G_M^{p(n)}(Q^2)}{G_M^3(Q^2)} \right)}{\int dQ^2 X(Q^2) F_A(Q^2) G_M^3(Q^2)} \\ & \left. \mp \frac{1}{2} \frac{\int dQ^2 X(Q^2) F_A(Q^2) G_M^s(Q^2)}{\int dQ^2 X(Q^2) F_A(Q^2) G_M^3(Q^2)} \right], \end{aligned} \quad (2.30)$$

where

$$X(Q^2) = \frac{Q^2}{p \cdot k} \left(1 - \frac{Q^2}{4p \cdot k} \right) \quad (2.31)$$

Let us stress that the integral asymmetry depends not only on the strange form factors, but also on the axial and electromagnetic form factors. In the scaling approximation, from Eq.(2.30) for the integral asymmetries we obtain

$$\begin{aligned} R_{p(n)} \mathbb{A}_{\langle \times \rangle} = & 1 \mp \frac{\int dQ^2 X(Q^2) F_A^s(Q^2) G_M^3(Q^2)}{\int dQ^2 X(Q^2) F_A(Q^2) G_M^3(Q^2)} \\ & \mp \frac{R_{p(n)}}{8|V_{ud}|^2} \frac{\int dQ^2 X(Q^2) F_A(Q^2) G_M^s(Q^2)}{\int dQ^2 X(Q^2) F_A(Q^2) G_M^3(Q^2)} \end{aligned} \quad (2.32)$$

where $R_p/8|V_{ud}|^2 = 1.11$ and $R_n/8|V_{ud}|^2 = 0.80$. Thus, also the integral asymmetries are very sensitive to the axial and vector strange form factors.

The integral asymmetry averaged over p and n obviously does not depend on the vector strange form factor and is given by the expression

$$A = \frac{\not{p}}{\not{p} |\not{V}_{\text{approx}}|} \left[\not{p} - \not{p} \sin^2 \theta_W + \not{p} \sin^2 \theta_W \frac{\int dQ^2 X(Q^2) F_A^s(Q^2) G_M^0(Q^2)}{\int dQ^2 X(Q^2) F_A(Q^2) G_M^3(Q^2)} \right]. \quad (2.33)$$

Thus, if it will turn out that the averaged integral asymmetry differs from the value $(1 - 2 \sin^2 \theta_W) / 4 |V_{ud}|^2$, it will be a model independent proof that the axial strange form factor is different from zero.

If form factor scaling takes place, for the averaged integral asymmetry we have

$$r A = 1 + 0.16 \frac{\int dQ^2 X(Q^2) F_A^s(Q^2) G_E^p(Q^2)}{\int dQ^2 X(Q^2) F_A(Q^2) G_E^p(Q^2)}. \quad (2.34)$$

III. DISCUSSION

From the data of the experiments on deep inelastic scattering of polarized leptons on polarized nucleons and from the data of other experiments it was found that the axial strange constant g_A^s is relatively large. These data led to an enormous amount of theoretical investigations and a big progress in the understanding of the structure of the nucleon [2]. Taking into account the importance of the “problem of the spin of the proton” and the theoretical uncertainties connected with the analysis of the data (small x extrapolation, violation of SU(3), etc.), it is very important to use other methods for the determination of the matrix elements of the strange currents.

The investigation of neutrino processes at relatively small Q^2 can be an important source of information about the matrix elements of the strange axial and vector currents [11].

We have considered the processes of elastic scattering of neutrinos and antineutrinos on nucleons. From the isotopic SU(2) invariance of strong interactions it follows that the cross sections of these processes are determined by the electromagnetic form factors of the proton and the neutron, by the axial CC form factor of the nucleon and by the strange vector and axial form factors. In order to minimize the uncertainties connected with the knowledge of the electromagnetic form factors of the neutron and, especially, of the axial form factor of the nucleon, we considered here the neutrino-antineutrino asymmetry \mathcal{A}_N determined by the relation (1.11). A measurement of the asymmetry \mathcal{A}_N would allow to obtain directly from the experimental data model independent informations on the strange vector and axial form factors of the nucleon.

In Section II we have shown that the asymmetry \mathcal{A}_N depends on the magnetic form factors of the proton and neutron, which are known with better accuracy than the electric ones. More specifically, the asymmetry \mathcal{A}_N depends on the ratio of the magnetic form factors of the neutron and proton. Rather detailed informations on the values of the proton form factors in a wide range of Q^2 (up to 30 GeV^2) were obtained from the data on elastic scattering of electrons on proton [16,17]. It was clearly shown that there is a deviation of the form factors from the dipole formula (up to 30% at high Q^2).

The values of the neutron form factors are much less known than those of the proton. A large part of the data on the neutron form factors were obtained from the analysis of quasi-elastic scattering of electrons on nuclei (in particular deuterium). This analysis requires the consideration of many theoretical effects (final state interaction, contributions of meson exchange currents, etc.). The values of these form factors in the range $1.75 \leq Q^2 \leq 4 \text{ GeV}^2$ were determined in a recent SLAC experiment [19]. Some informations on the value of G_M^n are also available in the region $4 \leq Q^2 \leq 10 \text{ GeV}^2$ [20]. However, it is necessary to keep in mind that the extraction of the value of G_M^n from the data in this region of Q^2 is based on a rather model dependent procedure.

The electromagnetic form factors of the nucleon enter into the relations (2.20) for the asymmetries through the ratios $R_{p(n)}(Q^2)$. We have considered these ratios for Q^2 values in the interval $0.5 \leq Q^2 \leq 10 \text{ GeV}^2$. In our calculations we have used the latest parameterizations of the electromagnetic form factors of the nucleon [21,22] that are aimed to describe all existing data. In order to calculate the ratios $R_{p(n)}(Q^2)$ with error bands, we have also done our own fit of the data on the nucleon form factors in the Q^2 region under consideration. For the magnetic form factor of the proton we have taken the following two-poles expression:

$$\frac{G_M^p}{\mu_p} = \frac{a_1}{1 + a_2 Q^2} + \frac{1 - a_1}{1 + a_3 Q^2} , \quad (3.1)$$

which was proposed in Ref. [23]. Taking into account possible violations of scaling, we have considered the following parameterization for the magnetic form factor of the neutron:

$$\frac{G_M^n}{\mu_n} = \frac{G_M^p}{\mu_p} \left(1 + a_4 Q^2 \right) . \quad (3.2)$$

In Eqs.(3.1) and (3.2) a_1, a_2, a_3, a_4 are variable parameters. From the fit of the data in the range $0.5 \leq Q^2 \leq 10 \text{ GeV}^2$ (114 proton points and 22 neutron points) we have obtained the following values for the parameters:

$$\begin{aligned} a_1 &= -0.50 \pm 0.04 , \\ a_2 &= 0.71 \pm 0.02 , \\ a_3 &= 2.20 \pm 0.04 , \\ a_4 &= -0.019 \pm 0.004 , \end{aligned} \quad (3.3)$$

with $\chi^2/\text{NDF}=163/132$, which corresponds to a confidence level of 3.5%. The magnetic form factors of the proton and neutron given by Eqs.(3.1)–(3.3) are presented in Figs.1 and 2 (solid line). In these figures the experimental data (circles with error bar) and the form factors calculated with the parameterizations of Refs. [21] and [22] are also presented (dashed and dot-dashed lines, respectively). It is seen from Figs.1 and 2 that in the considered region of Q^2 there is a good agreement between the different parameterizations of the form factors and the experimental data.

It is obvious that the parameterization given in Eqs.(3.1)–(3.3) is valid only in the limited Q^2 region in which we have performed the fit. We have also tried the parameterization

$$\frac{G_M^n}{\mu_n} = \frac{G_M^p}{\mu_p} \frac{1 + a_4 Q^2}{1 + a_5 Q^2} , \quad (3.4)$$

that provide the same behaviour for G_M^p and G_M^n at high Q^2 . However, the accuracy of the neutron data do not allow to determine the value of the parameter a_5 .

The results of our calculations for the ratios $R_p(Q^2)$ and $R_n(Q^2)$ are presented in Figs.3 and 4, respectively. The error bands correspond to a confidence level of 90%. In the same figures we have shown also the values of the ratios $R_p(Q^2)$ and $R_n(Q^2)$ calculated with the parameterizations of the form factors given in Refs. [21] and [22] (dashed and dot-dashed lines, respectively). The corresponding curves are contained within the above mentioned error bands, except in the region $Q^2 \lesssim 2 \text{ GeV}^2$. The error band that we have obtained for the ratios $R_p(Q^2)$ and $R_n(Q^2)$ is mainly due to the errors of the data on the neutron form factor. It is clear that better neutron data are needed.

Now we will discuss the strange form factors of nucleon. Some informations about the value of g_A^s were obtained from the analysis of the BNL data [13] on NC elastic scattering of neutrinos and antineutrinos on protons in the range $0.4 \leq Q^2 \leq 1.1 \text{ GeV}^2$. Under the assumptions that the contribution of the vector strange form factors can be neglected and that the axial strange form factor has the same dipole Q^2 behaviour as the non-strange one, the authors of Ref. [13] found $g_A^s = -0.15 \pm 0.09$, which is compatible with the value given in Eq.(1.6). The data from BNL were reanalyzed in Ref. [12]. In this paper the contributions of the strange axial as well as vector form factors were taken into account. Dipole formulas were assumed for both the vector and the axial strange form factors. The fitting parameters were g_A^s , $F_M^s(0) = \mu_s$, $\langle r_s^2 \rangle = -6 \left[\frac{dF_V^s(Q^2)}{dQ^2} \right]_{Q^2=0}$ and M_A (the axial cutoff mass). The following values for the parameters were obtained in their fit III (with $\chi^2/\text{NDF}=9.28/11$, corresponding to 60% CL): $g_A^s = -0.13 \pm 0.09$, $\mu_s = -0.39 \pm 0.70$, $\langle r_s^2 \rangle = -0.11 \pm 0.16 \text{ fm}^2$, $M_A = 1.049 \pm 0.023 \text{ GeV}$. They found, however, strong correlations between the values of M_A and g_A^s obtained from the fit. If $M_A = 1.086 \pm 0.015$, (which is the value that was obtained in the BNL experiment [13]), the data are well described under the assumption that $g_A^s = \mu_s = \langle r_s^2 \rangle = 0$ (with $\chi^2/\text{NDF}=14.12/14$, corresponding to 44% CL).

The strange vector form factors at small Q^2 were considered by Jaffe in Ref. [24]. This calculation is based on the vector dominance model (VDM). The contributions of ω , ϕ and one heavier meson were taken into account. A fit [25] of the nucleon isoscalar form factors was used and ω - ϕ mixing was considered. Large values for the strange matrix elements were obtained in this work ($-0.43 \leq \mu_s \leq -0.25$, $0.11 \leq \langle r_s^2 \rangle \leq 0.22$). The axial strange form factor was also calculated in the framework of VDM [27] taking into account the contributions of the isoscalar axial vector mesons $f_1(1285)$ and $f_1(1420)$.

Let us also notice that in accordance with the quark counting rule at high Q^2 , the axial and vector strange form factors must decrease more rapidly than the non-strange form factors:

$$F_i^s(Q^2) \sim \left(\frac{1}{Q^2} \right)^4 \quad (3.5)$$

A Q^2 dependence of the strange form factors stronger than the dipole one was in fact considered in Refs. [28,29] in analogy with the parameterization of the electric form factor of the neutron proposed in Ref. [30].

We have calculated the effect of the strange form factors on the asymmetries $\mathcal{A}_{\sqrt{(\lambda)}}$

determined by the relation (1.11) assuming some simple models. We would like to stress that these calculations can be considered only as illustrations of the possible effects of the strange form factors. We expect that some real information about the values of the strange form factors of the nucleon will be obtained in future neutrino experiments.

In Figs.5 and 6 the results of the calculation of quantities $4|V_{ud}|^2\mathcal{A}_p$ and $4|V_{ud}|^2\mathcal{A}_n$ as functions of Q^2 are shown. Here we have assumed that the axial and magnetic strange form factors are given by the dipole formulas

$$F_A^s(Q^2) = \frac{g_A^s}{\left(1 + \frac{Q^2}{M_A^{s2}}\right)^2}, \quad (3.6)$$

$$G_M^s(Q^2) = \frac{\mu^s}{\left(1 + \frac{Q^2}{M_V^{s2}}\right)^2}, \quad (3.7)$$

where $M_A^s = M_A$ and $M_V^s = M_V$, with the typical values $M_A = 1.032 \text{ GeV}$ and $M_V = 0.84 \text{ GeV}$. The shadowed areas in Figs.5 and 6 are due to the uncertainty of the electromagnetic form factors. These areas have been obtained under the assumption that $g_A^s = \mu_s = 0$. All the curves in Figs.5 and 6 have been obtained with $g_A^s = -0.15$. The dashed and dotted curves display the effect of axial strange form factor: they were obtained with $\mu_s = 0$ utilizing our fit and the WT2 fit, respectively, for the magnetic form factors of the nucleon. The solid and dot-dashed lines show the effect of the contribution of both the strange axial and vector form factors: they were obtained with $\mu_s = -0.3$ and utilizing our fit and the WT2 fit, respectively, for the magnetic form factors of the nucleon. The slow decrease of the asymmetry with Q^2 is due to the deviation of the electromagnetic form factors from the dipole behaviour. It is seen from Figs.5 and 6 that the contribution of the axial strange form factor to the asymmetries can be relatively large if the constant g_A^s has the value given by the EMC and other data. The combined effect of the axial and vector strange form factors depends on the signs of g_A^s and μ_s . If the signs of these constants are the same (as we have assumed), the contribution of the axial and vector strange form factors to the asymmetry add up. If the signs are opposite (as it is the case for example in Ref. [31]), the contribution of the vector strange form factor will compensate the contribution of the axial one.

Until now we considered a dipole-behaviour of the strange form factors. In the following we will calculate some values of the asymmetries $\mathcal{A}_{\sqrt{\langle \rangle}}$ in the case of a Q^2 -behaviour of the strange form factors weaker and stronger than the dipole. In Fig.7 we present some calculations of the quantity $R_p\mathcal{A}_{\sqrt{\langle \rangle}}$ as a function of Q^2 in the case of a high- Q^2 decrease of the strange form factors stronger than the dipole. For the strange form factors we have adopted the following formulas:

$$G_M^S(Q^2) = \frac{\mu_s}{\left(1 + \frac{Q^2}{M_V^2}\right)^2} \frac{1}{\left(1 + \lambda_M^s \frac{Q^2}{4M^2}\right)}, \quad (3.8)$$

$$F_A^s(Q^2) = \frac{g_A^s}{\left(1 + \frac{Q^2}{M_A^2}\right)^2} \frac{1}{\left(1 + \lambda_A^s \frac{Q^2}{4M^2}\right)}, \quad (3.9)$$

where λ_A^s and λ_M^s are unknown parameters. The dotted and dot-dashed curves in Fig.7 have been calculated with $\lambda_A^s = \lambda_M^s = 3$. The dotted and dashed line were calculated with $g_A^s = -0.15$, $\mu_s = 0$, whereas the dot-dashed and solid line with $g_A^s = -0.15$, $\mu_s = -0.3$. As it is seen from Fig.7, the contributions of the strange form factors to the asymmetry tend to disappear at high Q^2 but could be relatively large in low Q^2 region (at $Q^2 \lesssim 5 \text{ GeV}^2$ in the cases considered).

Finally, let us consider the case of a high- Q^2 decrease of the strange form factors weaker than the dipole. In order to improve the large Q^2 behaviour of the strange vector form factors proposed by Jaffe [24] we added one additional pole to his expressions for $F_V^s(Q^2)$ and $F_M^s(Q^2)$:

$$F_V^s(Q^2) = Q^2 \left[\frac{a_\omega}{Q^2 + m_\omega^2} + \frac{a_\phi}{Q^2 + m_\phi^2} + \frac{a_1}{Q^2 + m_1^2} + \frac{a_2}{Q^2 + m_2^2} \right], \quad (3.10)$$

$$F_M^s(Q^2) = \frac{b_\omega m_\omega^2}{Q^2 + m_\omega^2} + \frac{b_\phi m_\phi^2}{Q^2 + m_\phi^2} + \frac{b_1 m_1^2}{Q^2 + m_1^2} + \frac{b_2 m_2^2}{Q^2 + m_2^2}. \quad (3.11)$$

We have taken the values of the parameters that characterize the ω and ϕ poles and the third mass m_1 as in fit 8.1 of Ref. [24]. The value of the fourth mass was assumed to be $m_2 = 1.6 \text{ GeV}$ (which corresponds to a ω resonance). The other parameters in Eqs.(3.10) and (3.11) were fixed by imposing the following asymptotic conditions:

$$\begin{array}{ll} F_V^s(Q^2) \xrightarrow[Q^2 \rightarrow \infty]{} 0 & Q^2 F_M^s(Q^2) \xrightarrow[Q^2 \rightarrow \infty]{} 0 \\ Q^2 F_V^s(Q^2) \xrightarrow[Q^2 \rightarrow \infty]{} 0 & Q^4 F_M^s(Q^2) \xrightarrow[Q^2 \rightarrow \infty]{} 0 \end{array} \quad (3.12)$$

At $Q^2 = 0$ we have obtained $\langle r_s^2 \rangle = 0.055 \text{ fm}^2$ and $\mu_s = -0.14$, to be compared with the values $\langle r_s^2 \rangle = 0.11 \text{ fm}^2$ and $\mu_s = -0.25$ of Ref. [24].

For the axial strange form factor we have employed a dipole formula with a cutoff mass twice as large as M_A , which corresponds to a distribution of strange quarks inside of the nucleon narrower than the distributions of the u and d quarks (see Refs. [26,27]).

The results of our calculations of the quantity $R_p \mathcal{A}_p$ are shown in Fig.8. The increase of the asymmetry with Q^2 is due to the fact that the decrease of the strange form factors at high Q^2 is slower than that of the non-strange ones. Taking into account the fact that the asymptotical conditions for the strange form factors are more stringent than those for the non-strange form factors, we would like to warn that the behavior of the asymmetry presented in Fig.8 is strongly model dependent (at least at high Q^2).

In conclusion, we would like to make the following remark. In most neutrino experiments the interactions of neutrinos with nuclei are investigated. In order to obtain from these experiments some informations about the strange form factors of the nucleon, the nuclear effects must be taken into account. In the region of relatively large Q^2 ($Q^2 \gtrsim 0.5 \text{ GeV}^2$) in which we are interested, the relativistic Fermi gas approximation [32] can be used. It was shown in Ref. [29] that in the case of quasi-elastic electron-nuclei scattering this approximation works reasonably well. We plan to consider in detail the nuclear effects in our future work.

ACKNOWLEDGMENTS

It is a pleasure to thank M. Anselmino, J. Bernabeu, A. Marchionni and A. Pullia for fruitful discussions.

REFERENCES

- [1] J. Ashman *et al.*, Phys. Lett. B **206**, 364 (1988); Nucl. Phys. B **328**, 1 (1989).
- [2] M. Anselmino, A. Efremov and E. Leader, preprint CERN-TH/7216/94 (hep-ph@xxx.lanl.gov/9501369), April 1994, to appear in Phys. Rep.
- [3] D. Adams *et al.*, Phys. Lett. B **329**, 399 (1994).
- [4] K. Abe *et al.*, Phys. Rev. Lett. **74**, 346 (1995).
- [5] J. Kodaira *et al.*, Nucl. Phys. B **159**, 99 (1979); Nucl. Phys. B **165**, 129 (1979); Phys. Rev. D **20**, 627 (1979).
- [6] F. Close and R. Roberts, Phys. Lett. B **316**, 165 (1993).
- [7] J. Ellis and M. Karliner, Phys. Lett. B **341**, 397 (1995).
- [8] A.V. Efremov and O.V. Teryaev, JINR Report No. E2-88-287 (1988), unpublished; G. Altarelli and G.G. Ross, Phys. Lett. B **212**, 391 (1988).
- [9] S.D. Bass and P.V. Landshoff, Phys. Lett. B **336**, 537 (1994).
- [10] J. Lichtenstadt and H.J. Lipkin, preprint TAUP-2244-95 (hep-ph@xxx.lanl.gov/-9504277).
- [11] D.B. Kaplan and A. Manohar, Nucl. Phys. B **310**, 527 (1988); J. Ellis and M. Karliner, Phys. Lett. B **213**, 73 (1988).
- [12] G.T. Garvey, W.C. Louis and D.H. White, Phys. Rev. C **48**, 761 (1993).
- [13] L.A. Ahrens *et al.*, Phys. Rev. D **35**, 785 (1987).
- [14] K. Nishikawa, INS-Rep-924, April 1992; A.K. Mann *et al.*, BNL-PROPOSAL-889, Jan 1993; MINOS Coll., NuMI note NUMI-L-63, February 1995; NUMI-L-79, April 1995; ICARUS Coll., Gran Sasso Lab. preprint LNGS-94/99-I, May 1994.
- [15] Review of Particle Properties, Phys. Rev. D **50**, 1173 (1994).
- [16] L. Andivahis *et al.*, Phys. Rev. D **50**, 5491 (1994); R.G. Arnold *et al.*, Phys. Rev. Lett. **57**, 174 (1986); P.E. Bosted *et al.*, Phys. Rev. C **42**, 38 (1990); P.N. Kirk *et al.*, Phys. Rev. D **8**, 63 (1973); D.Krupa *et al.*, J. Phys. G **10**, 455 (1984).
- [17] W. Bartel *et al.*, Nucl. Phys. B **58**, 429 (1973).
- [18] K.M. Hanson *et al.*, Phys. Rev. D **8**, 753 (1973).
- [19] A. Lung *et al.*, Phys. Rev. Lett. **70**, 718 (1993).
- [20] S. Rock *et al.*, Phys. Rev. Lett **49**, 1139 (1982).
- [21] K. Watanabe and H. Takahashi, Phys. Rev. D **51**, 1423 (1995).
- [22] P.E. Bosted, Phys. Rev. C **51**, 509 (1995).
- [23] S.I. Bilen'kaya and Yu.M. Kazarinov, Sov. J. Nucl. Phys. **32**, 382 (1980).
- [24] R.L. Jaffe, Phys. Lett. B **229**, 275 (1989).
- [25] G. Höhler *et al.*, Nucl. Phys. B **224**, 505 (1976).
- [26] D.H. Beck, Phys. Rev. D **39**, 3248 (1989).
- [27] M. Kirchbach and H. Arenhövel, Contribution to the *Int. Conf. on Physics with GeV-Particle Beams*, 22-25 Aug 1994, Jülich, Germany (hep-ph@xxx.lanl.gov/9409293).
- [28] M.J. Musolf *et al.*, Phys. Reports **239**, 1 (1994).
- [29] T.W. Donnelly *et al.*, Nucl. Phys. A **541**, 525 (1992).
- [30] S. Galster, Nucl. Phys. B **32**, 221 (1971).
- [31] H. Weigel *et al.*, Phys. Lett. B **353**, 20 (1995).
- [32] C.J. Horowitz *et al.*, Phys. Rev. C **48**, 3078 (1993).

FIGURES

FIG. 1. Experimental data [16,17] of the proton magnetic form factor scaled by the dipole fit in the range $0.5 < Q^2 < 10 \text{ GeV}^2$ (circles with error bar). The fits given in Ref. [21] (dashed line), Ref. [22] (dot-dashed line) are shown together with our fit (solid line).

FIG. 2. Experimental data [17–20] of the neutron magnetic form factor scaled by the dipole fit in the range $0.5 < Q^2 < 10 \text{ GeV}^2$ (circles with error bar). The fits given in Ref. [21] (dashed line), Ref. [22] (dot-dashed line) are shown together with our fit (solid line).

FIG. 3. The value of the ratio R_p obtained with our fit of the proton and neutron magnetic form factors (solid line). The 90% confidence level region of R_p is depicted a shadowed band. The dashed and dot-dashed lines represent the values of R_p obtained with the fits given in Ref. [21] (WT2), Ref. [22] (Bosted), respectively. The dotted line represent the constant value of R_p in the scaling approximation.

FIG. 4. The value of the ratio R_n obtained with our fit of the proton and neutron magnetic form factors (solid line). The 90% confidence level region of R_n is depicted a shadowed band. The dashed and dot-dashed lines represent the values of R_n obtained with the fits given in Ref. [21] (WT2), Ref. [22] (Bosted), respectively. The dotted line represent the constant value of R_n in the scaling approximation.

FIG. 5. Plot of $4|V_{ud}|^2 \mathcal{A}_p$ as a function of Q^2 . The shadowed area corresponds to the uncertainty induced by the error of R_p (see Fig.3) in the absence of strange contributions. All the curves were obtained using a dipole form for $F_A^s(Q^2)$ with $g_A^s = -0.15$ and $M_A^s = M_A$. The dashed (dotted) curve was obtained with $G_M^S(Q^2) = 0$ utilizing our fit (the WT2 fit) for the magnetic form factors of the nucleon. The solid (dot-dashed) line was obtained using a dipole form for $G_M^S(Q^2)$ with $\mu_s = -0.3$, $M_V^s = M_V$ and utilizing our fit (the WT2 fit) for the magnetic form factors of the nucleon.

FIG. 6. Plot of $4|V_{ud}|^2 \mathcal{A}_n$ as a function of Q^2 . The shadowed area corresponds to the uncertainty induced by the error of R_n (see Fig.4) in the absence of strange contributions. All the curves were obtained using a dipole form for $F_A^s(Q^2)$ with $g_A^s = -0.15$ and $M_A^s = M_A$. The dashed (dotted) curve was obtained with $G_M^S(Q^2) = 0$ utilizing our fit (the WT2 fit) for the magnetic form factors of the nucleon. The solid (dot-dashed) line was obtained using a dipole form for $G_M^S(Q^2)$ with $\mu_s = -0.3$, $M_V^s = M_V$ and utilizing our fit (the WT2 fit) for the magnetic form factors of the nucleon.

FIG. 7. Plot of $R_p \mathcal{A}_p$ as a function of Q^2 . As in Fig.5, the shadowed area corresponds to the uncertainty induced by the error of R_p (see Fig.3) in the absence of strange contributions. The dashed and solid lines coincide with the corresponding lines of Fig.5. The dotted and dot-dashed curves were obtained with the Galster parameterization (3.8) and (3.9) for $G_M^s(Q^2)$ and $F_A^s(Q^2)$. The values of the parameters are: $g_A^s = -0.15$, $M_A^s = M_A$, $\lambda_A^s = \lambda_M^s = 3$, $M_V^s = M_V$, $\mu_s = 0$ and $\mu_s = -0.3$ for the dotted and dot-dashed curve, respectively.

FIG. 8. Plot of $R_p \mathcal{A}_p$ as a function of Q^2 . As in Figs.5 and 7, the shadowed area corresponds to the uncertainty induced by the error of R_p (see Fig.3) in the absence of strange contributions. All the curves were obtained using a dipole form for $F_A^s(Q^2)$ with $g_A^s = -0.15$. The dashed line, which was obtained with $G_M^s(Q^2) = 0$ and $M_A^s = M_A$, coincide with the corresponding line of Figs.5 and 7. The dotted line was obtained with $G_M^s(Q^2) = 0$ and $M_A^s = 2M_A$. The solid (dot-dashed) curve was obtained with the modified Jaffe parameterization for $G_M^s(Q^2)$ and $M_A^s = M_A$ ($M_A^s = 2M_A$).

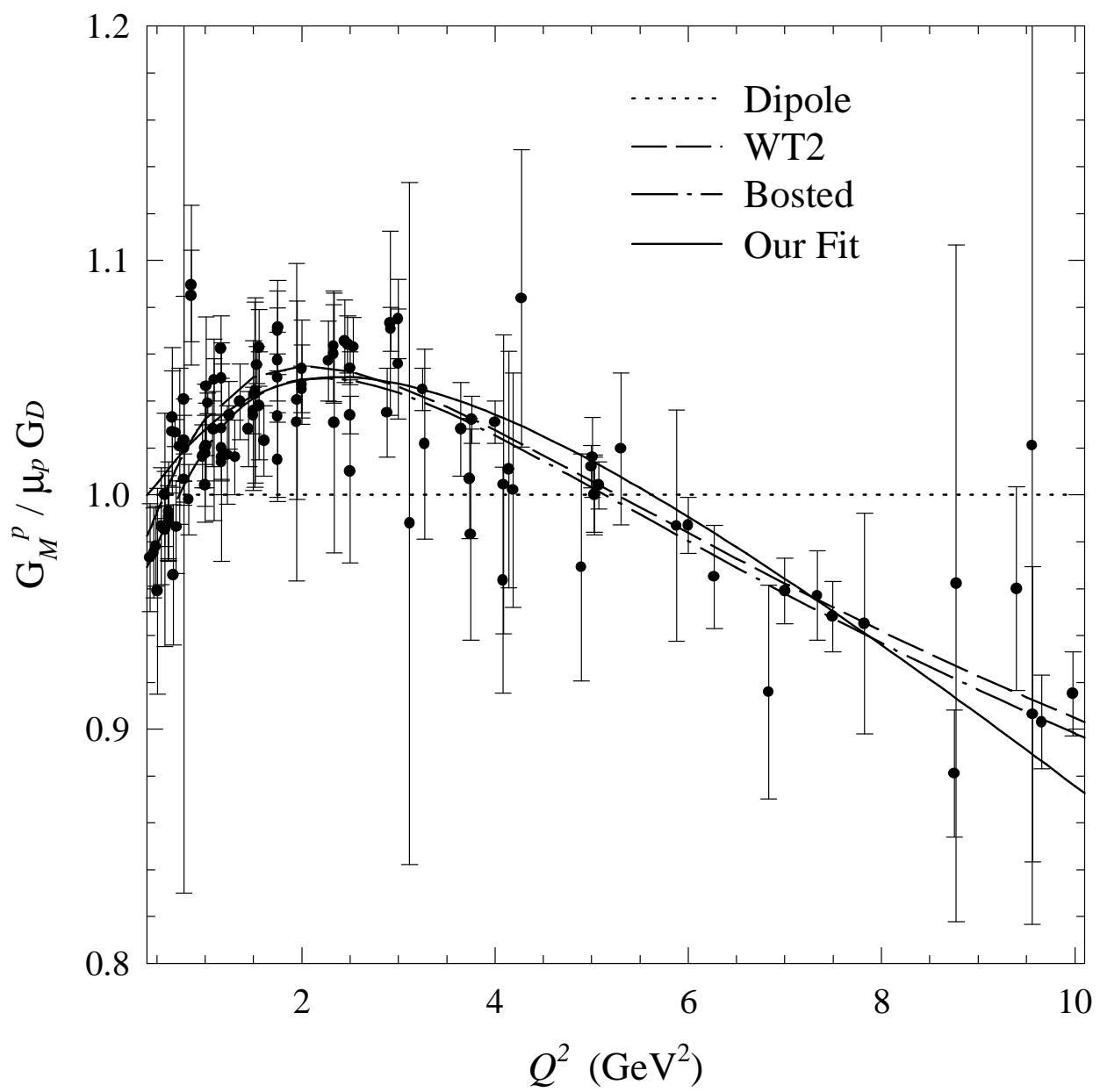


Figure 1

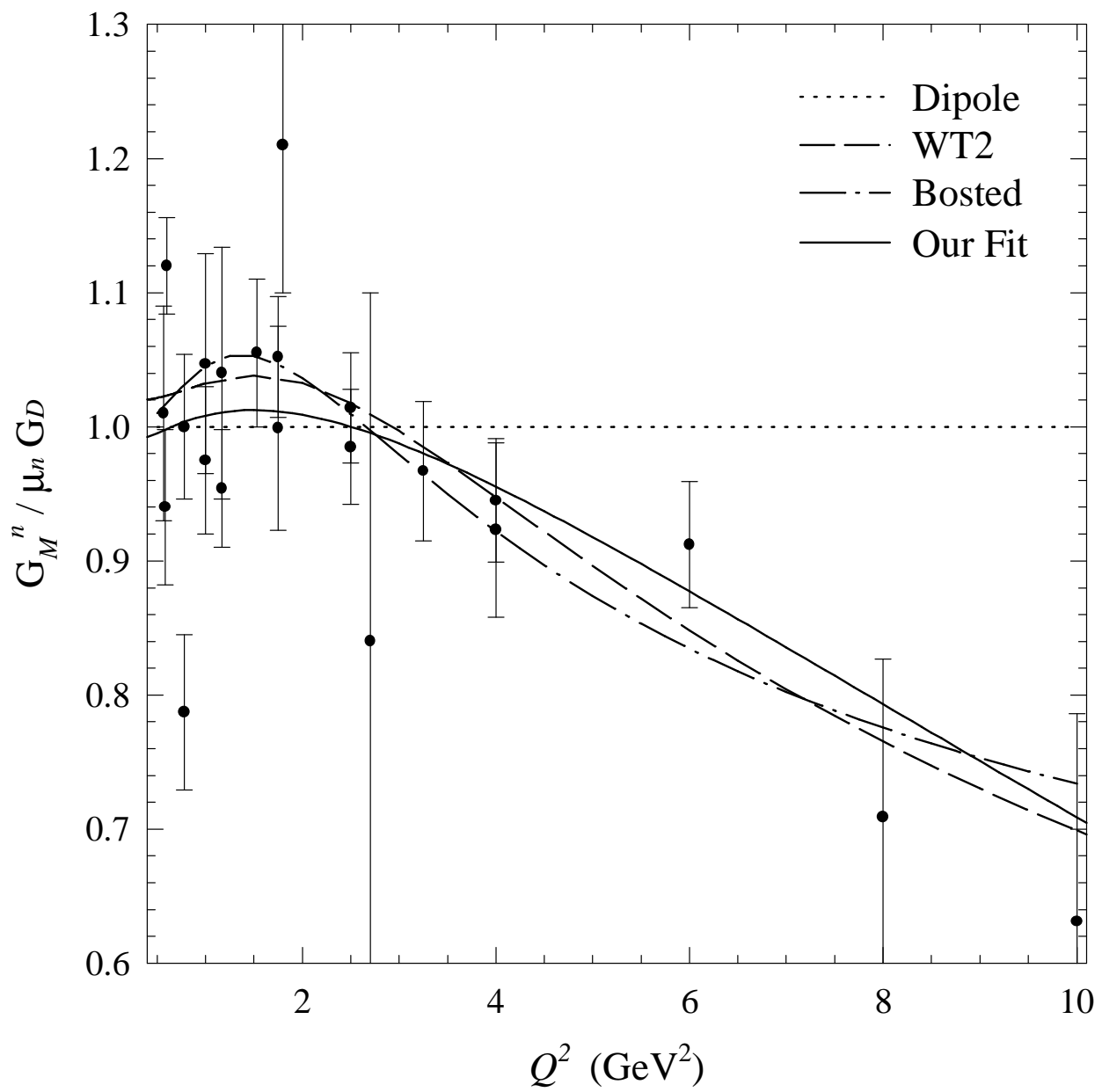


Figure 2

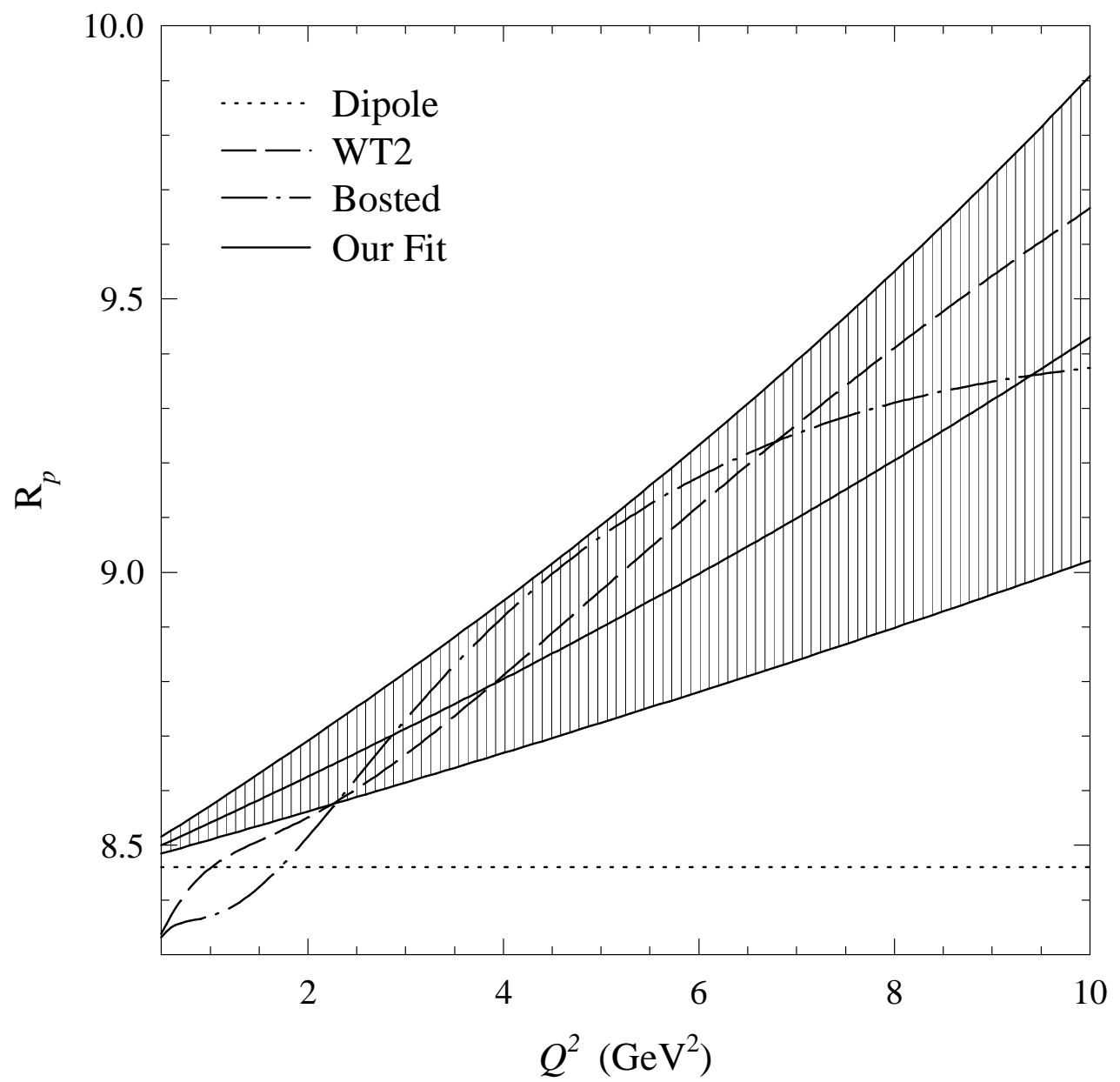


Figure 3

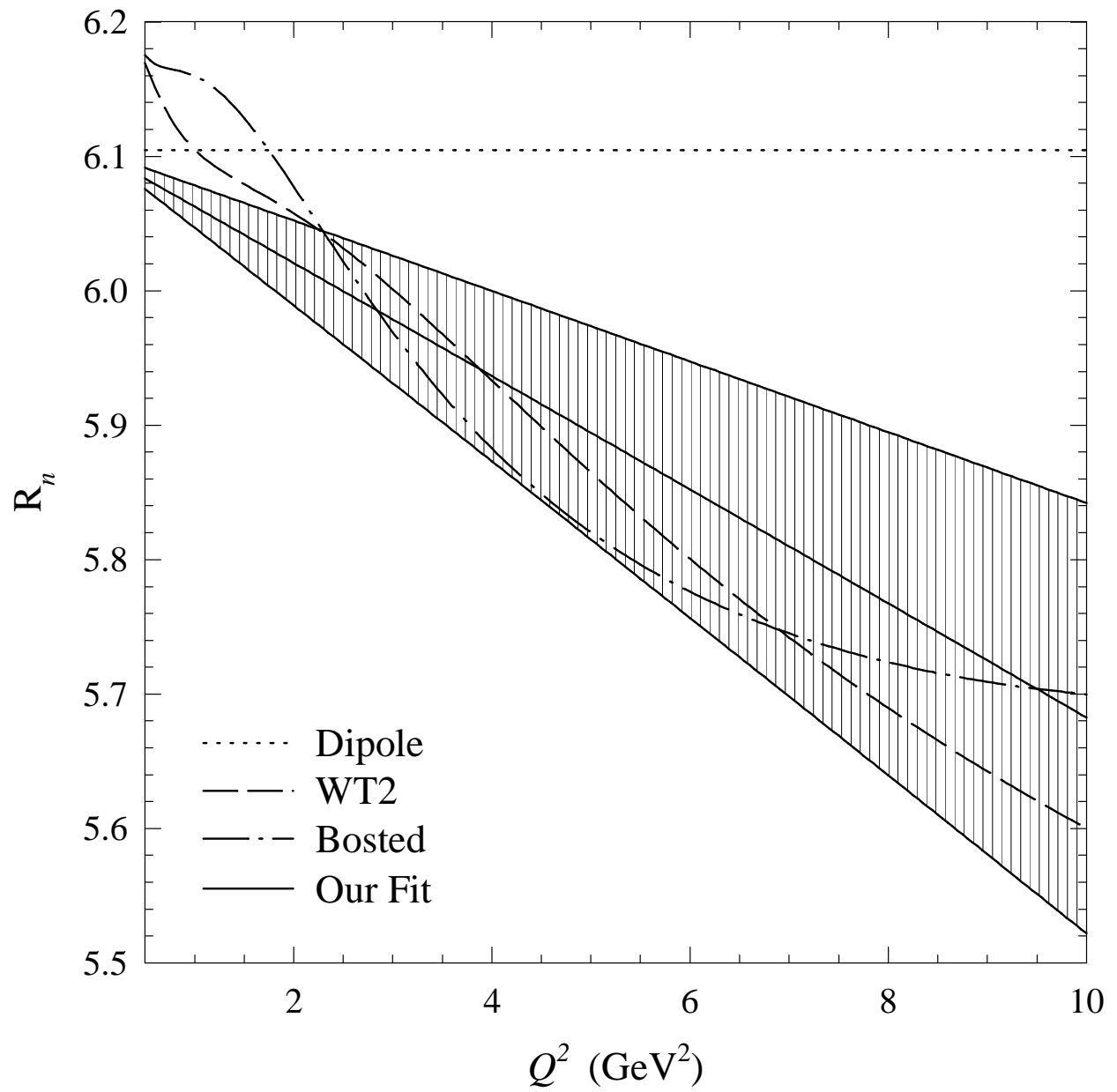


Figure 4

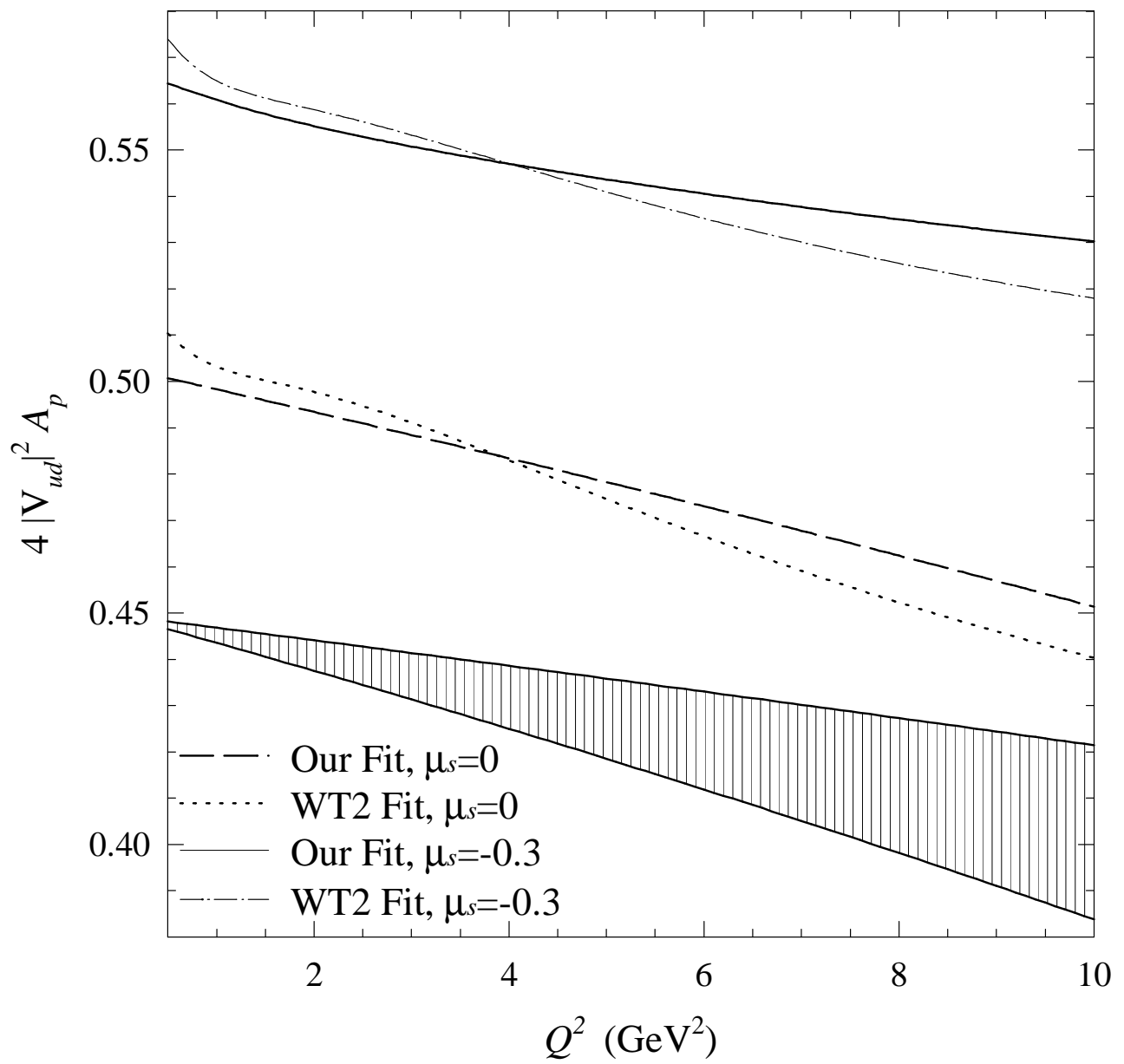


Figure 5

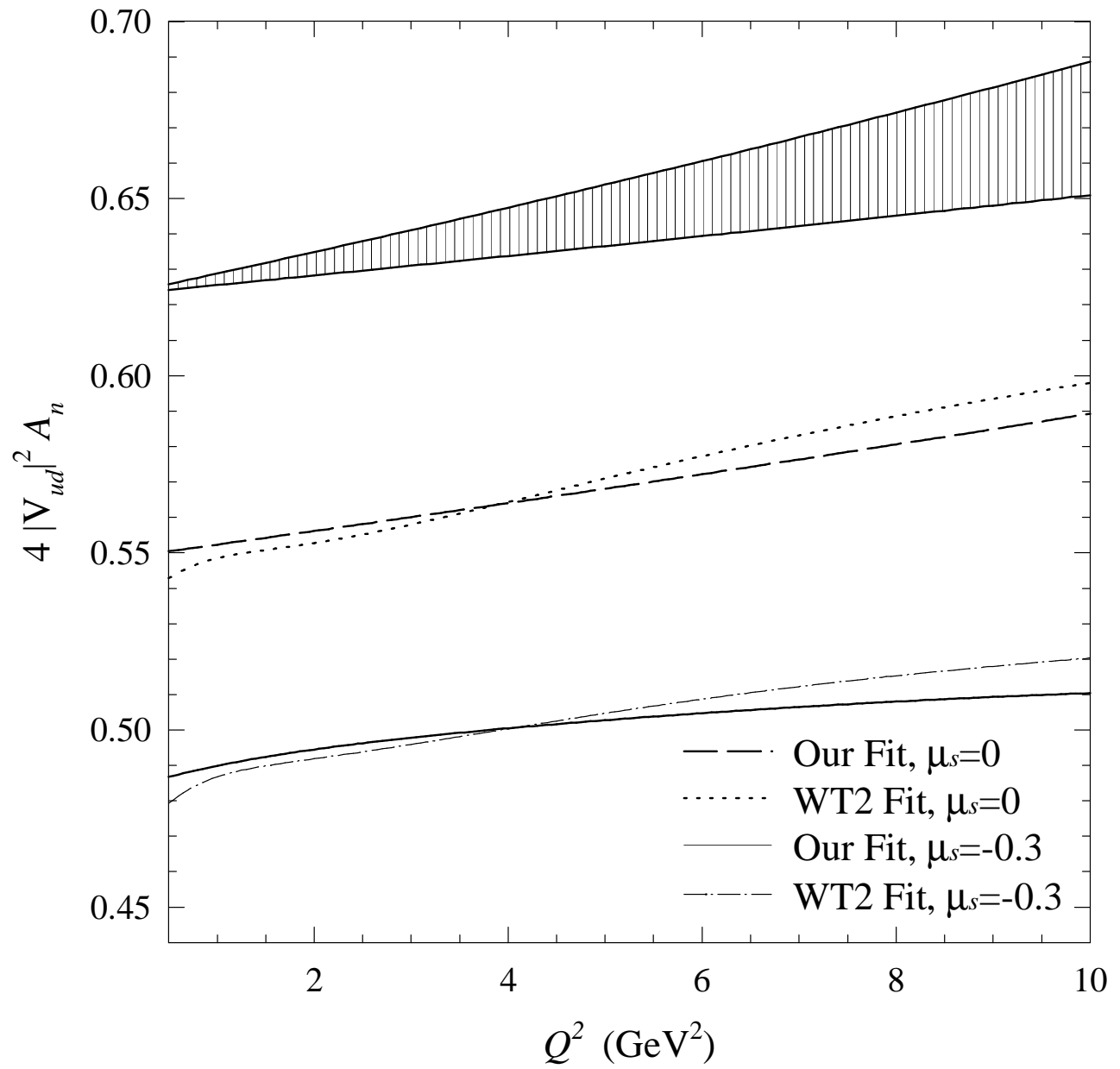


Figure 6

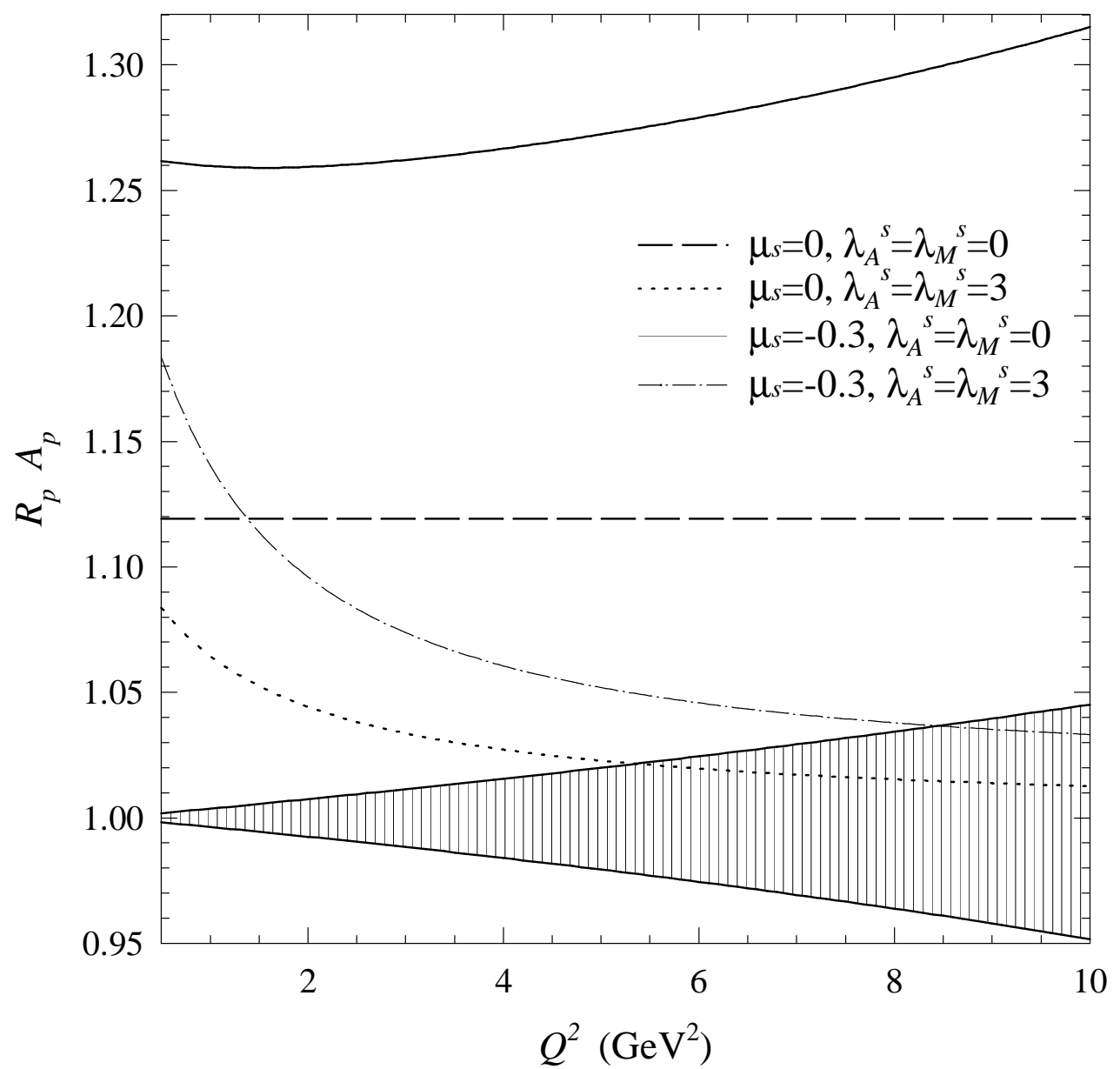


Figure 7

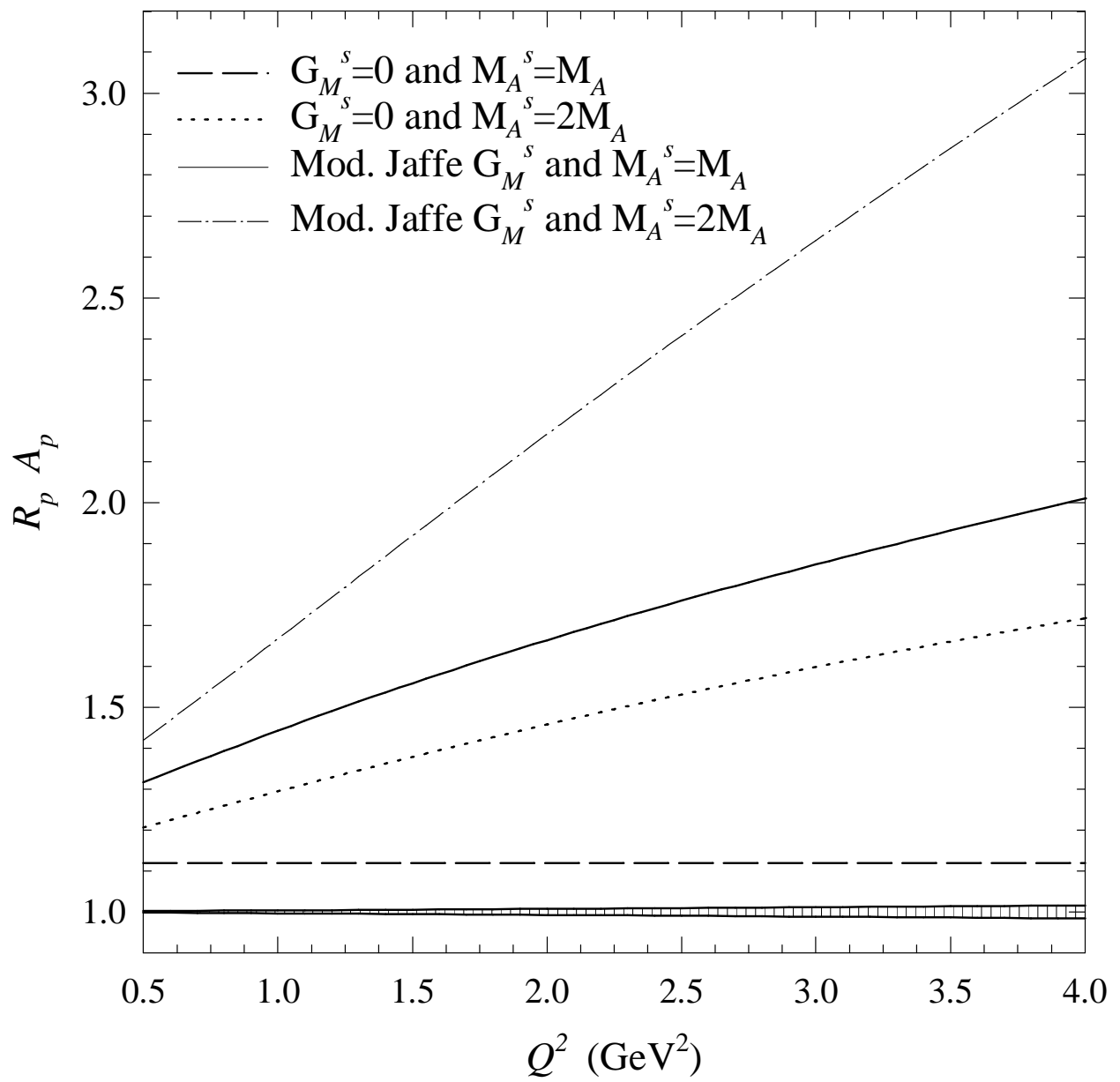


Figure 8